The Journal of Chemical Physics

Enhancing the understanding of the glycerol to lactic acid reaction mechanism over $AuPt/TiO_2$ under alkaline conditions

Cite as: J. Chem. Phys. **152**, 134705 (2020); https://doi.org/10.1063/1.5128595
Submitted: 21 September 2019 . Accepted: 09 March 2020 . Published Online: 07 April 2020

Christopher D. Evans, Mark Douthwaite, James H. Carter, Samuel Pattisson, Simon A. Kondrat, Donald Bethell, David W. Knight, Stuart H. Taylor, and Graham J. Hutchings

The Journal of Chemical Physics ARTICLE scitation.org/journal/jcp

Enhancing the understanding of the glycerol to lactic acid reaction mechanism over AuPt/TiO_2 under alkaline conditions

Cite as: J. Chem. Phys. 152, 134705 (2020); doi: 10.1063/1.5128595
Submitted: 21 September 2019 • Accepted: 9 March 2020 •
Published Online: 7 April 2020

Christopher D. Evans,[1] Mark Douthwaite,[1] James H. Carter,[1] Samuel Pattisson,[1] Simon A. Kondrat,[1,2,a)] Donald Bethell,[1] David W. Knight,[1] Stuart H. Taylor,[1] and Graham J. Hutchings[1,a)]

AFFILIATIONS

[1]Cardiff Catalysis Institute, School of Chemistry, Cardiff University, Main Building, Park Place, Cardiff CF10 3AT, United Kingdom
[2]Department of Chemistry, Loughborough University, Loughborough, Leicestershire, LE11 3TU, United Kingdom

Note: This paper is part of the JCP Special Topic Collection on Catalytic Properties of Model Supported Nanoparticles.
[a)]**Authors to whom correspondence should be addressed:** s.kondrat@lboro.ac.uk and hutch@cardiff.ac.uk

ABSTRACT

The oxidation of glycerol under alkaline conditions in the presence of a heterogeneous catalyst can be tailored to the formation of lactic acid, an important commodity chemical. Despite recent advances in this area, the mechanism for its formation is still a subject of contention. In this study, we use a model 1 wt. % AuPt/TiO_2 catalyst to probe this mechanism by conducting a series of isotopic labeling experiments with 1,3-^{13}C glycerol. Optimization of the reaction conditions was first conducted to ensure high selectivity to lactic acid in the isotopic labeling experiments. Selectivity to lactic acid increased with temperature and concentration of NaOH, but increasing the O_2 pressure appeared to influence only the rate of reaction. Using 1,3-^{13}C glycerol, we demonstrate that conversion of pyruvaldehyde to lactic acid proceeds via a base-promoted 1,2-hydride shift. There was no evidence to suggest that this occurs via a 2,1-methide shift under the conditions used in this study.

INTRODUCTION

Glycerol is a major by-product formed from the synthesis of first generation bio-fuels. Recent advances in this area, supported by substantial investment, has resulted in a significant increase in the quantity of glycerol produced per annum, and this is projected to further increase over the coming years. As such, the market value of glycerol has decreased markedly, and an abundance of glycerol is available.[1]

The highly functionalized nature of glycerol allows for many different valorization strategies. One such strategy involves the aerobic oxidation of glycerol over noble metal supported catalysts, which can result in the formation of many different value-added products (Scheme 1). Since Rossi and Prati[2] first established that supported Au catalysts were highly active for the aerobic oxidation of alcohols, much research has been published on the oxidation of glycerol.[3,4] The complexity of the product distribution, formed from various parallel and sequential processes, makes this reaction an interesting model system for the study of heterogeneous catalysis; a deeper understanding of the influence of different metals, support properties, and particle size effects has been established.[3,5–7]

The current understanding is that the reaction, as shown in Scheme 1, involves an initial oxidation of an alcohol function to carbonyl, producing a mixture of reaction intermediates: dihydroxyacetone (DHA) or glyceraldehyde (GLD). This mixture reacts further via two competing pathways, further oxidation or dehydration. Unraveling the factors that promote each of the pathways is difficult since the initial alcohol oxidation is considered to be the rate determining step (RDS).[8] The further oxidation pathway converts the GLD or DHA sequentially into glyceric acid (GA) and tartronic acid (TA). However, an additional competitive pathway arises from GA, which involves the scission of C–C bonds, which many attribute to the *in situ* formation of H_2O_2.[9] This can allow for the formation of C_2 and C_1 oxidation products such as glycolic acid (GLO),

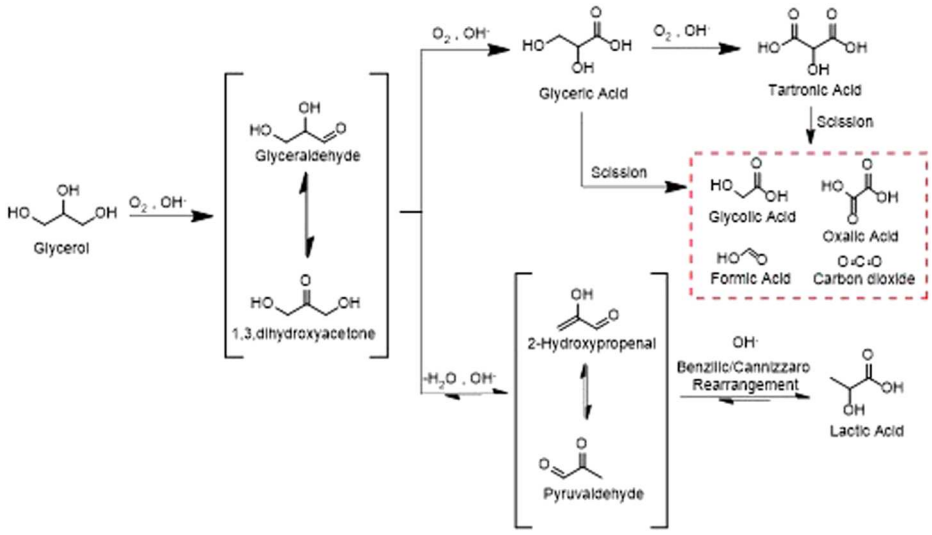

SCHEME 1. Reaction scheme illustrating the different products which can form during the aerobic oxidation of glycerol in alkaline conditions over noble metal supported catalysts. The red dotted lines correspond to products formed from scission of either glyceric acid or tartronic acid.

oxalic acid (OA), and formic acid (FA). By contrast, if dehydration is favored, pyruvaldehyde (PALD) or its corresponding enol is formed. PALD can then undergo a rearrangement to produce lactic acid (LA). The nature of this rearrangement reaction remains a subject of much debate; various publications have suggested that this proceeds via a 1,2-hydride shift, commonly referred to as an intramolecular Cannizzaro reaction,[10,11] while others propose a 2,1-methide shift, analogous to a benzilic acid rearrangement.[12]

Of the reaction products described, the conversion of glycerol into LA has perhaps generated the most interest in recent years. LA can be used as a reagent to produce ethyl lactate, a common biodegradable solvent, and as a monomer used to produce the bioplastic polylactic acid.[13] The development of such polymers has perhaps become even more pressing in recent years due to plastic wastes infiltrating ecosystems all over the world. This has rightly led to very public concerns and mounted pressure on the plastics industry to develop greener and more sustainable products. Many studies have uncovered catalysts that can provide high selectivity to LA from glycerol conditions, and developments made in this area were recently documented in an in-depth review.[14]

Under base-free conditions, the initial alcohol oxidation is followed by Brønsted acid catalyzed dehydration of a primary alcohol; many reports have aligned reaction selectivity to LA with this catalytic property.[6] However, there is much evidence to suggest that Lewis acid sites are responsible for the rearrangement from PALD to LA.[15,16] Interestingly, reaction selectivity to LA also improves as the quantity of base in the system increases,[17] suggesting that the dehydration of the GLD is favored over its direct oxidation to GA. The influence of the catalyst on this dehydration reaction under these conditions remains elusive. DHA and GLD, although never observed under alkaline conditions, are considered to exist in equilibrium;[18] the rate of isomerization between these two compounds is influenced by pH.[19] As such, it is likely that the proportion of these two compounds in solution and how they interact with the catalyst are ultimately what dictates reaction selectivity.

In this study, we use isotopic labeling experiments to confirm the reaction mechanism for the formation of LA from PALD using 1,3-^{13}C glycerol. High LA selectivity during this study is ensured by a thorough optimization of reaction conditions in the presence of a model 1 wt. % AuPt/TiO_2 catalyst. These optimization reactions also led to important conclusions regarding the competitive mechanisms that take place on the catalyst surface; GLD and DHA can either undergo catalytic oxidation to GA and TA or dehydration to PALD.

EXPERIMENTAL

Materials (source and purity)

Acetic acid (Sigma-Aldrich, ≥99.7%); chloroauric acid (Strem, 99.8%); chloroplatinic acid hexahydrate (Sigma-Aldrich, ACS reagent, 37.5% Pt basis); formic acid (Sigma-Aldrich, ≥98%); glyceric acid (TCI, 40 wt. % in water); glycerol (Sigma-Aldrich, ≥99.5%); glycolic acid (Sigma-Aldrich, 99%); concentrated hydrochloric acid (Fisher Scientific, ~37%); lactic acid (Sigma-Aldrich, 85 wt. % in H_2O); concentrated nitric acid (Fisher Scientific, 70%); oxalic acid (Sigma-Aldrich, ≥99.99%); phosphoric acid (Sigma-Aldrich, 85 wt. % in H_2O); polyvinylalcohol (Sigma-Aldrich, 80% hydrolyzed); pyruvic acid (Sigma-Aldrich, 98%); sodium borohydride (Sigma-Aldrich, 99.99%); sodium hydroxide (Fischer Scientific, 99.3%); concentrated sulfuric acid (Fisher Scientific, >95%); tartronic acid (Sigma-Aldrich, ≥97%); Titania P25 (Degussa, ≥99.5%); and water (Fisher Scientific, HPLC grade).

Definitions

$$Conversion(\%) = \frac{Mol\ of\ glycerol\ converted}{Initial\ mol\ of\ glycerol} \times 100. \quad (1)$$

Equation (1): Expression to calculate the conversion of glycerol in a typical glycerol oxidation experiment. Conversion is expressed as a

percentage.

$$Selectivity\ of\ product\ A\ (\%) = \frac{Mol\ of\ product\ A}{Mol\ of\ reactant\ converted} \times 100. \quad (2)$$

Equation (2): Expression to calculate reaction selectivity to a given product, in this case product A, in a typical glycerol oxidation experiment. Selectivity is expressed as a percentage.

$$Carbon\ mass\ balance\ (\%) = \frac{Mol\ of\ carbon\ from\ glycerol_{START}}{Total\ mol\ of\ carbon} \times 100. \quad (3)$$

Equation (3): Expression to calculate the carbon mass balance (CMB) in a given glycerol oxidation experiment. Moles of carbon from $glycerol_{START}$ correspond to the number of moles of carbon present at the start of the reaction. Total moles of carbon correspond to the sum of the carbon moles in reaction products and residual glycerol in a given sample.

Catalyst preparation

The model 1 wt. % Au–Pt/TiO_2 catalyst was prepared by the sol-immobilization methodology, using polyvinyl alcohol (PVA) as the stabilizing agent. The experimental procedure used for the synthesis of the catalyst (2 g) is as follows: $HAuCl_4$ (0.82 ml, 12.25 g/l) and H_2PtCl_6 (2.052 ml, 4.85 g/l) were added to a beaker (1 l) containing H_2O (800 ml) and a magnetic stirrer. Aqueous PVA (1.3 ml, from 0.1 g PVA in 10 ml H_2O) was subsequently added and left to stir for 15 min. Freshly prepared aqueous $NaBH_4$ (3.928 ml, 0.2M) was then added instantaneously to the solution, forming a yellow/gray sol. The mixture was then stirred for 30 min before acidification to pH 2, through the dropwise addition of concentrated H_2SO_4. Powdered TiO_2 (1.98 g) was added, and the solution was stirred for an additional 1 h. The resulting mixture was then filtered under vacuum, washed with de-ionized water (2 l), and dried in a conventional fan oven (16 h, 110 °C). The recovered solid was ground into a powder using an agate mortar and pestle.

Glycerol oxidation

All catalyst testing was conducted using a Radley's starfish reactor using the following experimental procedure: To a round bottom flask (50 ml), aqueous glycerol solution (10 ml, 0.6M), aqueous NaOH (10 ml, 0.6–2.4M), AuPt/TiO_2 (58.2 mg), and a magnetic stirrer were added. The flask was subsequently sealed, purged three times with the reactant gas, and charged with the desired pressure of O_2 or He (0.5–4 barg). The gas inlet remained open over the duration of the experiments to ensure that the system was maintained at the desired pressure. The flask was then secured to the reactor, which had been preheated to the desired reaction temperature (40–120 °C). Once secured, the magnetic stirring (1000 RPM) and reaction timer were initiated. In some reactions, 0.5 ml samples were taken at specific intervals (typically 30 min, 60 min, 120 min, and 240 min). For this process, the flask was removed and cooled with an ice bath prior to de-pressurization. Once the sample was taken, the same purging and charging procedure was repeated, and the flask was re-secured to the reactor. The samples taken from the reactions were immediately diluted tenfold in de-ionized water to quench the reaction and were subsequently filtered. Quantification of the samples was conducted using an Agilent 1260 Infinity HPLC equipped with ultraviolet and refractive index detectors using an external calibration method. The products were separated at 50 °C, over a Metacarb 67H column using an isocratic mobile phase of aqueous H_3PO_4 (0.1 wt. %, flow rate = 0.6 ml min^{-1}).

Catalyst characterization

Brunauer Emmett Teller (BET) surface area measurements were conducted using a Quadrasorb surface area analyzer. A 5-point isotherm of each material was measured using N_2 as the adsorbate gas. Samples were degassed at 250 °C for 2 h prior to analysis.

Transmission electron microscopy (TEM) was carried out with a Jeol 2100 with a LAB6 filament operating at 200 kV. Each sample was prepared by dispersing the powdered catalyst in ethanol and dropping the suspension onto a lacey carbon film over a 300 mesh copper grid.

The metal loading of the catalyst was determined by Microwave Plasma–Atomic Emission Spectrometry (MP-AES). For this, catalyst (50 mg) was added to a volumetric flask (50 ml) containing freshly prepared *aqua regia* (5 ml), ensuring the sample was fully submerged in the liquid. The catalyst was then left for 24 h to ensure full dissolution of metal after which the flask was filled to 50 ml with de-ionized water. The solution was subsequently filtered using a polytetrafluoroethylene (PTFE) syringe filter (0.45 μm) to remove any residual particulates. The liquid effluent was then analyzed using an Agilent 4100 MP-AES. A series of solutions were made using Au (Agilent, 1000 ppm) and Pt (Agilent, 1000 ppm) standards. The calibrations and reaction effluent was subsequently analyzed at multiple wavelengths for each element to ensure accuracy.

The ^{13}C and ^{1}H NMR spectra were obtained using a Bruker Avance 400 MHz DPX spectrometer. The chemical shifts for ^{1}H NMR were run in deuterated chloroform ($CDCl_3$) or deuterated dimethylsulfoxide (d_6-DMSO).

RESULTS AND DISCUSSION

Synthesis and characterization of the model AuPt/TiO_2 catalyst

Previous publications have reported that supported AuPt catalysts are effective for the aerobic oxidation of glycerol to LA under alkaline conditions.[17] Despite this, the mechanism for the formation of LA remains elusive. Derivation of the mechanism for this transformation is crucially important as such detail can be fed back into catalyst design. For this reason, we synthesized a 1 wt. % AuPt/TiO_2 catalyst by the sol-immobilization method to use as a model to study the mechanism in this reaction. This technique was used because it is highly reproducible and typically produces supported metal catalysts with narrow particle size distributions (PSDs).[20]

TEM was performed on the synthesized catalyst to confirm that it possessed the desired dispersion of AuPt. Images from this characterization and the corresponding PSDs are displayed in Fig. 1. The data demonstrate that the Au and Pt are, indeed, well dispersed in this catalyst. Here, a mean particle size of 1.68 nm was calculated with a standard deviation of 0.78 nm using a representative sample

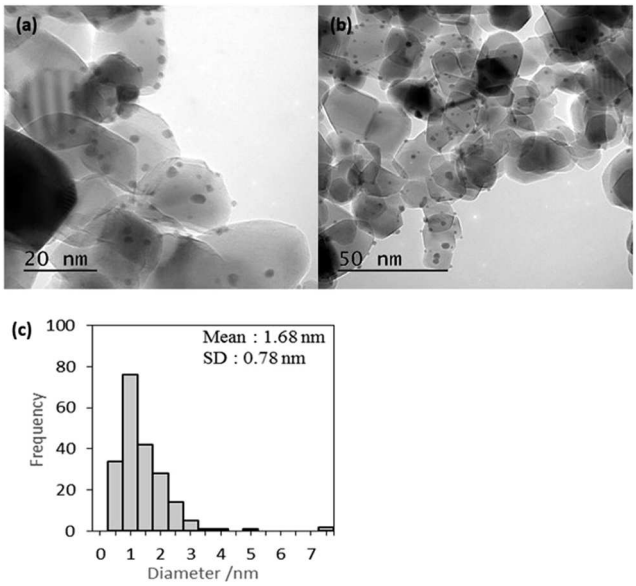

FIG. 1. Transmission electron micrographs of the model AuPt/TIO$_2$ catalyst prepared by sol-immobilization: (a) 20 nm inset and (b) 50 nm inset. (c) A histogram evidencing the size distribution of the supported AuPt particles.

size. Previously, Peneau *et al.*[21] confirmed using aberration corrected microscopy that the particles in AuPt/TiO$_2$ catalysts, prepared using the same methodology, predominantly consist of alloyed Au and Pt. To ensure that the catalyst synthesized in this study consisted of the desired quantity of Au and Pt, a known quantity of the catalyst was digested in *aqua regia*, and the resulting solution was analyzed by MP-AES. The results confirmed that the catalyst has a total AuPt loading of 0.98 wt. % and a molar ratio of 1:0.91 (Au:Pt). BET surface area analysis confirmed that the final catalyst exhibited a surface area of 61 m^2 g^{-1}, which is within the typical range of commercial Degussa TiO$_2$–P25.[22]

Investigation into the influence of reaction conditions on the 1 wt. % AuPt/TiO$_2$ catalyst

Prior to the mechanistic investigation, the reaction conditions were first optimized to ensure that the isotopic labeling experiments were conducted under conditions that favor high LA selectivity. From the observations made by Heeres and co-workers[17] over a 1 wt. % AuPt/CeO$_2$ catalyst, it is known that the reaction temperature, pH, and O$_2$ pressure can influence the product distribution although a detailed understanding and explanation of how these parameters affect the reaction mechanism has not been reported. It was, therefore, important to conduct similar optimization reactions using our model AuPt/TiO$_2$ catalyst.

TABLE I. The influence of the reaction temperature on the glycerol conversion and selectivity profile of the reaction products, over the model AuPt/TiO$_2$ catalyst. **Reaction conditions:** 10 ml reaction volume, glycerol (0.3M), NaOH (0.6M), O$_2$ pressure (1 barg), metal:substrate ratio of 1000:1, 4 h reaction time, and reaction temperature (40–120 °C). **Key:** CMB (carbon mass balance); GA (glyceric acid); TA (tartronic acid); C–C scission (oxalic acid, formic acid, and glycolic acid); and LA (lactic acid).

				Selectivity (%)			
Temperature (°C)	Time (min)	Conversion (%)	CMB (%)	GA	TA	C–C scission	LA
40	30	24	100	65	3	21	11
	60	48	99	66	3	19	12
	120	89	100	64	5	21	10
	240	100	100	63	5	21	11
60	30	30	101	62	3	12	23
	60	59	99	61	5	13	21
	120	92	98	61	6	14	19
	240	100	100	59	7	16	18
80	30	28	100	38	6	11	45
	60	64	99	36	8	11	45
	120	97	99	35	11	8	46
	240	100	100	31	15	6	48
100	30	32	99	20	8	4	68
	60	68	101	16	10	5	69
	120	100	98	12	15	5	68
	240	100	100	10	16	6	68
120	30	45	95	16	9	4	71
	60	88	87	14	8	6	72
	120	100	80	12	10	6	72
	240	100	76	11	11	8	70

The performance of the 0.98 wt. % AuPt/TiO_2 catalyst in this reaction was assessed over time at different temperatures, which evidently had a significant impact on both the activity and selectivity [Table I, Fig. 2(a)]. As discussed previously, the reaction pathway leading to the formation of LA competes directly with a parallel oxidation route. As the reaction temperature is increased, the selectivity to LA increases at the expense of GA, TA, and C–C scission products. The activity of the catalyst also clearly increases with reaction temperature, which is also reflected in the proportion of TA:GA; at higher reaction temperatures, a larger proportion of GA undergoes sequential oxidation to TA. Interestingly, reaction selectivity to C–C scission products decreases as the reaction temperature increases. LA is fairly stable under these reaction conditions, even at high temperatures. The maximum LA selectivity is observed at a reaction temperature of 120 °C; however, under these conditions, there is a significant drop in the associated CMB. The highest yield of LA (~68%) is, therefore, observed at 100 °C.

Following these experiments, the effect of O_2 pressure on the product distribution and catalytic activity was investigated [Table II, Fig. 2(b)]. Davis and co-workers previously demonstrated that O_2 plays an indirect role in the oxidation of glycerol.[23] It was established that O_2 from the gas phase is not incorporated into the reaction products and concluded that the role of O_2 is to act as an electron scavenger, removing electron density from the surface of the supported metal particles to liberate active sites. This is also evidenced in Table II; under an inert atmosphere, the rate of glycerol dehydrogenation is extremely low. Interestingly, as the O_2 pressure is increased from 0.5 barg to 2 barg, a non-proportional increase in the rate of glycerol dehydrogenation is observed. This evidences that under such conditions, O_2 is unlikely to be chemically involved in the RDS, which is consistent with the observations by Davis and co-workers. Interestingly, under higher O_2 pressure (2–4 barg), the rate of dehydrogenation appears to be far more dependent on O_2 pressure, which may be indicative of a change in both the reaction mechanism and role of O_2 in the RDS.

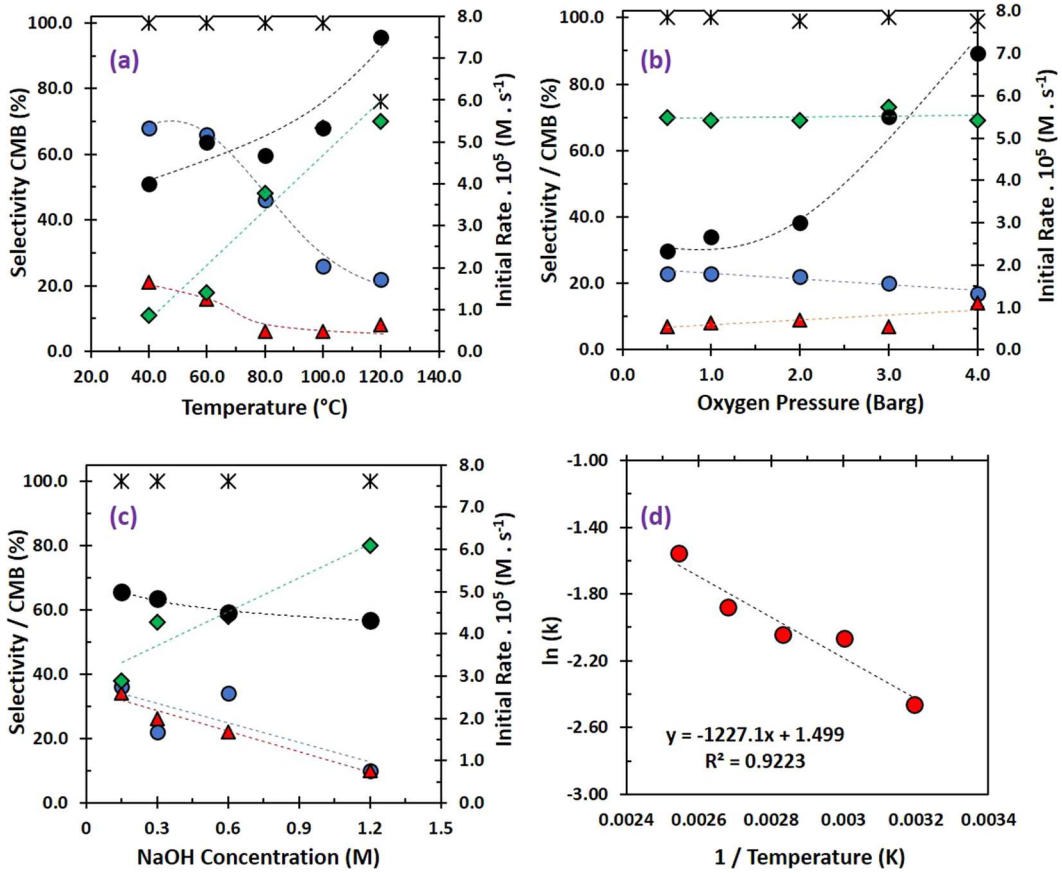

FIG. 2. The influence of temperature (a), O_2 pressure (b), and NaOH concentration (c) on the reaction selectivity, carbon mass balance, and initial rate for the oxidation of glycerol over the 1 wt. % AuPt/TiO_2 catalyst. The Arrhenius plot (d) is used to calculate the experimental activation energy for glycerol oxidation. To ensure fair comparison, the data points in (a)–(c) are collected at iso-conversion; conversion = 100% for (a), 72%–84% for (b), and 100% for (c). The initial rate data were generated after 30 min (1800 s) of reaction. Key: Initial rate—black circle; lactic acid selectivity—green diamond; direct oxidation selectivity—blue circle; C–C scission selectivity—red triangle; and Carbon Mass Balance—black asterisk. Note: Selectivity to direct oxidation products is the sum of reaction selectivity to glyceric and tartronic acid.

TABLE II. The influence of O_2 pressure on the glycerol conversion and selectivity profile of the reaction products over the model AuPt/TiO_2 catalyst. **Reaction conditions:** 10 ml reaction volume, glycerol (0.3M), NaOH (0.6M), O_2 (0.5–4 barg)—**He*** corresponds to reaction run under 3 barg of He, metal:substrate ratio of 1000:1, 4 h reaction time, and 100 °C. **Key:** CMB (carbon mass balance); GA (glyceric acid); TA (tartronic acid); C–C scission (oxalic acid, formic acid, and glycolic acid); and LA (lactic acid).

				Selectivity/%			
Oxygen pressure (barg)	Time (min)	Conversion (%)	CMB (%)	GA	TA	C–C scission	LA
He*	30	1	100	40	0	0	60
	60	1	100	34	0	7	59
	120	2	100	18	0	23	59
	240	3	100	10	1	30	59
0.5	30	14	100	26	0	1	73
	60	28	100	25	0	4	71
	120	67	101	24	1	5	70
	240	78	100	22	1	7	70
1.0	30	16	101	25	0	3	72
	60	36	99	24	1	5	70
	120	72	100	22	1	8	69
	240	88	101	21	2	9	68
2.0	30	18	100	24	0	6	70
	60	44	101	23	1	8	68
	120	84	99	20	2	9	69
	240	94	100	17	3	11	69
3.0	30	33	100	20	1	5	74
	60	73	100	19	1	7	73
	120	96	99	15	2	11	72
	240	100	101	12	4	13	71
4.0	30	42	100	16	1	11	72
	60	79	99	15	2	14	69
	120	100	97	14	3	18	65
	240	100	95	5	12	18	65

As the pressure of O_2 is increased from 0.5 barg to 3 barg, reaction selectivity to LA remains fairly constant. At 4 barg, the selectivity to LA begins to drop, which becomes more apparent as the reaction proceeds. Interestingly, reaction selectivity to GA and TA also drops as the pressure of O_2 is increased. Only reaction selectivity to C–C cleavage products appears to increase consistently as the pressure of O_2 increases. The sum of reaction selectivity to GA, TA, and the products of C–C remains fairly constant across all O_2 pressures. This suggests that (i) O_2 promotes the C–C scission pathway and (ii) the C–C scission either occurs from GA or TA or competes with the oxidation of GLD to GA. Many publications have previously attributed C–C cleavages in these reactions to the *in situ* formation of H_2O_2.[9,24] Given that the formation of hydrogen peroxide intermediates is likely to be a product of an oxygen reduction reaction with H_2O, it is reasonable to suggest that increasing the pressure of O_2 in the system would indeed result in an increased rate of H_2O_2 formation. The notable drop in CMB at 4 barg could indicate that the resultant products that arise from these cleavages are further oxidized to CO_2, which is not included in our analytical procedure.

After establishing that reaction selectivity to LA is optimum at 100 °C and 3 barg of O_2, it is important to understand how influential the pH of the system was on the product distribution. Due to the strength of the O–H bond under base-free conditions, this process is typically considered to be rate-determining.[25] This hypothesis is supported by the data in Table III as the concentration of NaOH in the reaction appears to have no observable influence on the rate of reaction. However, under base-free conditions, the rate of reaction is substantially lower. The rate of glycerol dehydrogenation is, therefore, independent of NaOH concentration. Thereafter, competition exists between sequential oxidation to GA and the base catalyzed dehydration to PALD. Both these pathways involve $^-$OH, but only the rate of dehydration appears to be dependent on its concentration.

TABLE III. The influence of NaOH concentration on the glycerol conversion and selectivity profile of the reaction products over the model AuPt/TiO_2 catalyst. **Reaction conditions:** 10 ml reaction volume, glycerol (0.3 M), NaOH (0–1.2M), O_2 pressure (3 barg), metal:substrate ratio of 1000:1, 4 h reaction time, and 100 °C. **Key:** CMB (carbon mass balance); GA (glyceric acid); TA (tartronic acid); C–C scission (oxalic acid, formic acid, and glycolic acid); LA (lactic acid); and DHA (dihydroxyacetone).

NaOH concentration (M)	Time (min)	Conversion (%)	CMB (%)	Selectivity (%)				
				GA	TA	DHA	LA	C–C scission
0	30	1	99	10	1	79	0	10
	60	5	100	8	1	67	0	24
	120	8	100	7	2	61	0	30
	240	11	100	5	3	58	0	34
0.15	30	30	100	42	4	0	35	19
	60	64	100	41	5	0	36	18
	120	97	99	35	7	0	37	21
	240	100	100	28	8	0	38	26
0.3	30	29	99	28	4	0	55	13
	60	59	100	25	7	0	54	14
	120	92	100	18	9	0	55	18
	240	100	100	8	14	0	56	22
0.6	30	27	99	29	2	0	68	9
	60	55	100	27	7	0	65	10
	120	88	100	29	12	0	58	14
	240	100	100	16	18	0	58	13
1.2	30	26	100	16	2	0	78	4
	60	52	99	11	6	0	78	5
	120	78	100	5	8	0	79	8
	240	100	100	0	10	0	80	10

From the data presented in Tables I–III and Fig. 2, it is evident that the reaction conditions are exceptionally influential on the reaction selectivity over our model catalyst. Further evaluation of the initial rates under various NaOH and O_2 pressures allowed for the derivation of a rate equation for the oxidation of glycerol. Evidently, under the optimized reaction conditions, the reaction is first order with respect to O_2 and zero order with respect to NaOH. Through assumption that the reaction is first order with respect to glycerol, the total order of the reaction and the rate equation may be expressed as $K = k\,.\,\text{cat.}\,[\text{Glycerol}]^1[O_2]^1[\text{NaOH}]^0$. Following an established method,[26,27] it was possible to quantify the concentration of dissolved O_2 in the alkaline aqueous solutions at the different temperatures. This allowed for (i) the determination of the corresponding rate constants, (ii) the construction of an Arrhenius plot, and (iii) determination of the activation energy (E_a). The experimental activation energy calculated for the oxidation of glycerol over the 1 wt. % AuPt/TiO_2 catalyst was 10.2 kJ mol^{-1} under these conditions. This is notably lower than other examples from the literature of Au supported catalysts for glycerol oxidation. Activation energies of 57 kJ mol^{-1}, 50 kJ mol^{-1}, and 35 kJ mol^{-1} have been confirmed experimentally for the oxidation of glycerol over Au supported on Al_2O_3, C, and MoO_3/γ–Al_2O_3, respectively.[28–30] However, it is well established that AuPt/TiO_2 catalysts are substantially more active than monometallic Au catalysts for this reaction,[31] which could provide explanation for the lower activation energy observed in this study.

The highest selectivity to LA at full conversion was ~83%, which was achieved at 100 °C, in the presence of 1.2M of NaOH and 3 barg O_2 pressure (Table IV). To further understand the role of the catalyst in the formation of LA, some additional experiments were conducted from DHA, GLD, and PALD (Table V). In the presence of the catalyst, selectivity to LA is either equal to or slightly lower than that observed in the absence of catalyst. Furthermore, each reaction conducted in the presence of the heterogeneous catalyst leads to the formation of pyruvic acid (PA). The CMB for these reactions are notably lower than those observed in Tables I–III, which is likely to be attributed to additional bimolecular pathways that occur. Based on all the aforementioned results, we can propose an updated scheme (Scheme 2).

Under alkaline conditions, glycerol adsorbs through either its primary or secondary alcohol group leading to the formation of the corresponding surface alkoxy intermediate. From the primary alkoxy intermediate, abstraction of an adjacent hydrogen leads to the desorption of GLD. GLD can then either re-adsorb and undergo a sequential oxidation to produce TA or is consumed in a homogeneous base catalyzed dehydration reaction to produce 2-hydroxypropenal (the enol form of PALD). GA can evidently be produced from GLD via base promoted reactions in the presence

TABLE IV. The substrate conversion and the selectivity profile of the reaction products that are formed in a reaction over the model AuPt/TiO_2 catalyst under optimized reaction conditions. **Reaction conditions:** 10 ml reaction volume, glycerol (0.3M), NaOH (1.2M), O_2 pressure (3 barG), metal:substrate ratio of 1000:1, 4 h reaction time, and 100 °C. **Key:** CMB (carbon mass balance); GA (glyceric acid); TA (tartronic acid); C–C scission (oxalic acid, formic acid, and glycolic acid); LA (lactic acid); PA (pyruvic acid); DHA (dihydroxyacetone); GLD (glyceraldehyde); and PALD (pyruvaldehyde).

Substrate	Time (min)	Conversion (%)	Carbon balance (%)	Selectivity (%)			
				GA	TA	C–C scission	LA
Glycerol	30	31	99	14	2	3	81
	60	56	100	9	4	5	82
	120	89	100	6	4	7	83
	240	100	100	5	4	8	83
1,3-Di-^{13}C glycerol	30	28	99	14	2	5	79
	60	49	100	11	4	7	78
	120	85	100	8	4	9	79
	240	100	100	7	4	10	79

TABLE V. The aerobic oxidation of dihydroxyacetone, glyceraldehyde, and pyruvaldehyde in the presence and absence of the model AuPt/TiO_2 catalyst under basic conditions. **Reaction conditions:** 10 ml reaction volume, substrate (0.1M), NaOH (0.4M), O_2 pressure (3 barg), metal:substrate ratio of 1000:1, 0.5 h reaction time, and 100 °C. **Key**: CMB (carbon mass balance); GA (glyceric acid); TA (tartronic acid); C–C scission (oxalic acid, formic acid, and glycolic acid); LA (lactic acid); and PA (pyruvic acid); DHA (dihydroxyacetone); GLD (glyceraldehyde); and PALD (pyruvaldehyde).

Substrate	Catalyst	Conv. %	Selectivity (%)					CMB (%)
			GA	TA	C–C scission	LA	PA	
DHA	Yes	98	15	6	24	51	4	52
	No	97	20	3	25	52	0	57
GLD	Yes	100	18	8	26	46	2	66
	No	100	18	3	27	53	0	62
PALD	Yes	100	0	0	5	92	4	97
	No	100	0	0	5	96	0	88

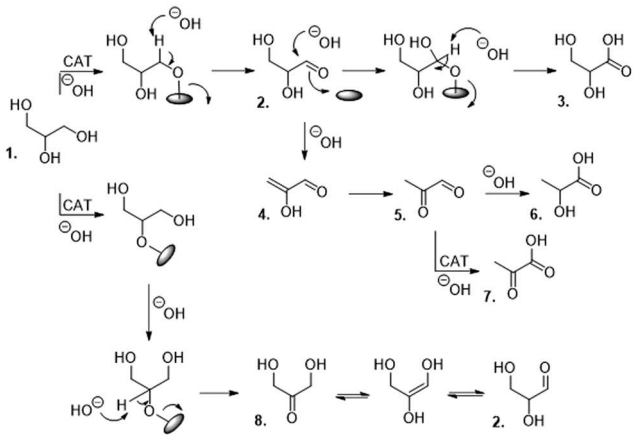

SCHEME 2. Proposed mechanisms for the transformation of glycerol under alkaline conditions. 1. glycerol, 2. glyceraldehyde, 3. glyceric acid, 4. 2-hydroxypropenal, 5. pyruvaldehyde, 6. lactic acid, 7. pyruvic acid, and 8. dihydroxyacetone.

and absence of the catalyst. This is evidenced by a slight increase in selectivity to GA and TA observed in the catalyzed and blank reactions, which utilize GLD as the substrate. The 2-hydroxypropenal produced through this dehydration tautomerizes to PALD, which can subsequently undergo a base catalyzed rearrangement to LA or is oxidized to PA, over the catalyst.

Insight on the mechanistic pathway to lactic acid from glycerol

After dehydration of GLD, there are two possible routes by which PALD can proceed to LA: via a 2,1-methide shift [Scheme 3(a)] or a 1,2-hydride shift [Scheme 3(b)]. Both of these reactions are promoted by –OH and do not appear to be influenced by the presence of our heterogeneous catalyst (Table V). Fortunately, distinguishing which of these two mechanisms is dominant in our system is possible as the 2,1-methide shift results in the migration of a carbon atom. As such, the position of the carbon atoms in the starting glycerol would be altered in the LA product.

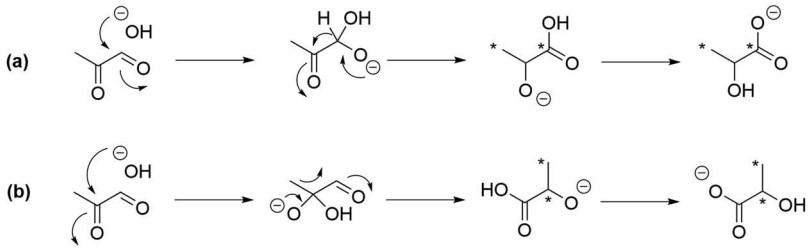

SCHEME 3. Mechanisms for the base catalyzed transformation of pyruvaldehyde to lactic acid. Under alkaline conditions, lactic acid may be produced via (a) a 1,2-hydride shift or (b) 2,1-methide shift. * is used to illustrate the location of ^{13}C isotopes in lactic acid for each reaction mechanism.

To determine which of the mechanisms occur, some additional experiments were conducted using isotopically labeled ^{13}C glycerol (1,3-di-^{13}C, 99 atom %) in the presence of our model catalyst. This isotopic compound was selected for these experiments as the formation of LA with ^{13}C in the second position would indicate that the reaction proceeds via a 2,1-methide shift. To ensure that the performance of our model catalyst was comparable using this labeled compound, a standard reaction was conducted under the optimized reaction conditions (Table IV). The performance was comparable to that observed with glycerol; a slight drop in the rate of reaction and LA selectivity is observed with the 1,3-di-^{13}C glycerol, which might evidence a very minor kinetic isotope effect. Nevertheless, the important conclusion to draw from these experiments is that the model 0.98 wt. % catalyst behaves in largely the same way with both substrates, and thus, we can be confident that the post dehydration reaction mechanism is the same.

Following this, samples from the reaction with 1,3-di-^{13}C glycerol at time = 0 min, 60 min, and 240 min were probed by ^{13}C NMR, and the corresponding spectra are displayed in Fig. 3. At 0 h, prior to reaction [Fig. 3(a)], only one significant ^{13}C signal is observed at a chemical shift (δ) of 62 ppm. The shift in this region is characteristic of a ^{13}C atom bonded to a hydroxide group. After 60 min of reaction, two additional signals appear in the ^{13}C NMR spectrum [Fig. 3(b)]. In addition to the ^{13}C shift at 62 ppm, significant signals are observed at δ = 20 and 182 ppm. The shift at δ = 20 ppm is characteristic of a ^{13}C atom in an alkyl group and, given the quantitative analysis in Table IV, can be assigned to the methyl group in LA. The shift at δ = 182 ppm is somewhat more difficult to assign, as a shift in this region can be indicative of a ^{13}C atom double bonded to an oxygen atom in either a carbonyl or carboxylic acid group. Under alkaline conditions, however, aldehydic products are not observed in this reaction, and given that only trace quantities of pyruvic acid and no mesoxalic acid are observed, we can confidently assign this signal to the ^{13}C atom in a carboxylic acid group in LA. After 240 min of reaction [Fig. 3(c)], the spectrum is dominated by signals at δ = 20 and 182 ppm. Some additional signals are also observed, which likely correspond to some of other by-products formed in the reaction. If the reaction had proceeded via the alternative mechanism, a 2,1-methide shift, a dominant signal at δ = 182 ppm would not be observed.

Given that ^{13}C signals can be assigned to both the methyl and carboxylic acid component in LA, which appear to be in similar quantities, the mechanism to LA from PALD cannot proceed via a 2,1-methide shift and must, therefore, proceed through a 1,2-hydride shift. Had the alternative mechanism operated, the labeled LA would have adjacent ^{13}C atoms and, hence, appear as doublets

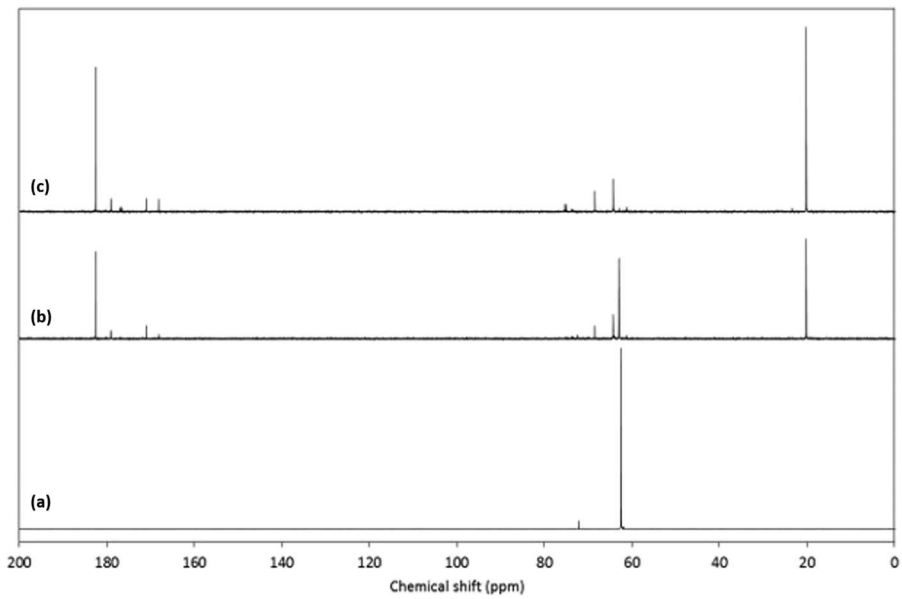

FIG. 3. NMR spectra corresponding to reactions of 1,3-di-^{13}C glycerol over the AuPt/TiO_2 catalyst after 0 min (a), 60 min (b), and 240 min (c). Reaction conditions: 10 ml reaction volume, glycerol (0.3M), NaOH (1.2M), O_2 pressure (3 barg), metal:substrate ratio of 1000:1, and reaction temperature (100 °C).

(*J ca*. 50 Hz). Instead, we observe very clean singlets in these proton-decoupled spectra. Had the alternative product been formed, then a large resonance at *ca*. 70 ppm [for the labeled CH(OH) group] would be expected, which is essentially absent. This is not necessarily surprising; while both the carbonyls in PALD activate each other to nucleophilic attack, the aldehyde is more reactive as the ketone has an additional electron-donating methyl group attached, making it less electrophilic and, thus, less susceptible to undergo nucleophilic attack.

CONCLUSION

A model AuPt/TiO_2 catalyst was used to study the reaction mechanisms that occur in the transformation of glycerol to LA under alkaline conditions. The reaction conditions were highly influential on both the rate of glycerol conversion and the product distribution. The catalyst is required for the oxidative dehydrogenation of glycerol to a mixture of DHA and GLD. GLD can subsequently partake in a sequential oxidation reaction to GA and undergo C–C scission or dehydration to 2-hydroxypropenal, which tautomerizes to PALD. There was no evidence to suggest that the heterogeneous catalyst was involved in any of the reactions leading from GLD to LA. Isotopic labeling experiments using ^{13}C glycerol were subsequently conducted and confirmed that PALD undergoes a base catalyzed 1,2-hydride shift to form LA. We consider the results and discussion herein and alleviate some uncertainty within the literature, providing clarity on the mechanisms taking place in this reaction and the role of the catalyst.

REFERENCES

[1] U. I. Nda-Umar, I. Ramli, Y. H. Taufiq-Yap, and E. N. Muhamad, Catalysts **9**, 15 (2019).
[2] L. Prati and M. Rossi, J. Catal. **176**, 552 (1998).
[3] G. Dodekatos, S. Schünemann, and H. Tüysüz, ACS Catal. **8**, 6301 (2018).
[4] C.-H. Zhou, J. N. Beltramini, Y.-X. Fan, and G. Q. Lu, Chem. Soc. Rev. **37**, 527 (2008).
[5] Y. Wang, Y. Xiao, and G. Xiao, Chin. J. Chem. Eng. **27**, 1536 (2019).
[6] A. Villa, N. Dimitratos, C. E. Chan-Thaw, C. Hammond, L. Prati, and G. J. Hutchings, Acc. Chem. Res. **48**, 1403 (2015).
[7] N. Razali and A. Z. Abdullah, Appl. Catal. A Gen. **543**, 234 (2017).
[8] J. Fu, Q. He, P. J. Miedziak, G. L. Brett, X. Huang, S. Pattisson, M. Douthwaite, and G. J. Hutchings, Chem.: A Eur. J. **24**, 2396 (2018).
[9] D. Wang, A. Villa, D. Su, L. Prati, and R. Schlögl, ChemCatChem **5**, 2717 (2013).
[10] H. Yin, C. Zhang, H. Yin, D. Gao, L. Shen, and A. Wang, Chem. Eng. J. **288**, 332 (2016).
[11] H. Yin, H. Yin, A. Wang, L. Shen, Y. Liu, and Y. Zheng, J. Nanosci. Nanotechnol. **17**, 1255 (2017).
[12] D. Roy, B. Subramaniam, and R. V. Chaudhari, ACS Catal. **1**, 548 (2011).
[13] S. A. Zavrazhnov, A. L. Esipovich, S. M. Danov, S. Y. Zlobin, and A. S. Belousov, Kinet. Catal. **59**, 459 (2018).
[14] R. Abdullah, S. N. Mohamed Saleh, K. Embong, and A. Z. Abdullah, Chem. Eng. Commun. **1**, 1 (2019).
[15] Z. Tang, S. L. Fiorilli, H. J. Heeres, and P. P. Pescarmona, ACS Sustainable Chem. Eng. **6**, 10923 (2018).
[16] K. M. A. Santos, E. M. Albuquerque, G. Innocenti, L. E. P. Borges, C. Sievers, and M. A. Fraga, ChemCatChem **11**, 3054 (2019).
[17] R. K. P. Purushothaman, J. van Haveren, D. S. van Es, I. Melián-Cabrera, J. D. Meeldijk, and H. J. Heeres, Appl. Catal. B Environ. **147**, 92 (2014).
[18] V. A. Yaylayan, S. Harty-Majors, and A. A. Ismail, Carbohydr. Res. **318**, 20 (1999).
[19] R. W. Nagorski and J. P. Richard, J. Am. Chem. Soc. **123**, 794 (2001).
[20] A. Villa, D. Wang, G. M. Veith, F. Vindigni, and L. Prati, Catal. Sci. Technol. **3**, 3036 (2013).
[21] V. Peneau, Q. He, G. Shaw, S. A. Kondrat, T. E. Davies, P. Miedziak, M. Forde, N. Dimitratos, C. J. Kiely, and G. J. Hutchings, Phys. Chem. Chem. Phys. **15**, 10636 (2013).
[22] X. Wang, S. O. Pehkonen, J. Rämö, M. Väänänen, J. G. Highfield, and K. Laasonen, Catal. Sci. Technol. **2**, 784 (2012).
[23] B. N. Zope, D. D. Hibbitts, M. Neurock, and R. J. Davis, Science **330**, 74 (2010).
[24] W. C. Ketchie, M. Murayama, and R. J. Davis, Top. Catal. **44**, 307 (2007).
[25] Q. Gu, P. Sautet, and C. Michel, ACS Catal. **8**, 11716 (2018).
[26] W. Xing, G. Yin, and J. Zhang, *Rotating Electrode Methods and Oxygen Reduction Electrocatalysts* (Elsevier, 2014).
[27] A. Schumpe, I. Adler, and W.-D. Deckwer, Biotechnol. Bioeng. **20**, 145 (1978).
[28] J. Díaz, E. Skrzyńska, J.-S. Girardon, M. Capron, F. Dumeignil, and P. Fongarland, ChemEngineering **1**, 7 (2017).
[29] S. Demirel, M. Lucas, J. Wärnå, T. Salmi, D. Murzin, and P. Claus, Top. Catal. **44**, 299 (2007).
[30] T. A. Ntho, P. Gqogqa, and J. L. Aluha, *Advanced Chemical Kinetics* (IntechOpen, 2018).
[31] A. Villa, A. Jouve, F. J. Sanchez Trujillo, D. Motta, L. Prati, and N. Dimitratos, Catalysts **8**, 54 (2018).